

Fig. 2: Frequency response of reflection coefficient.

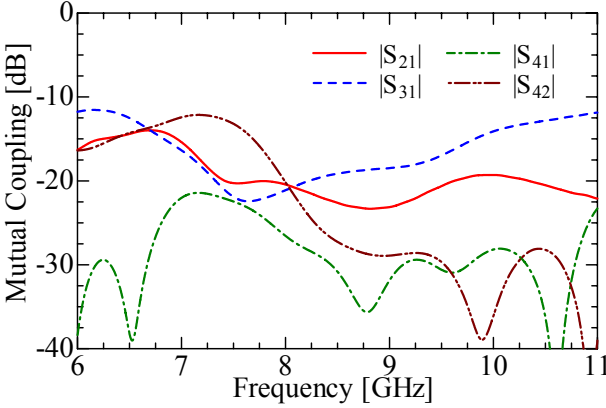


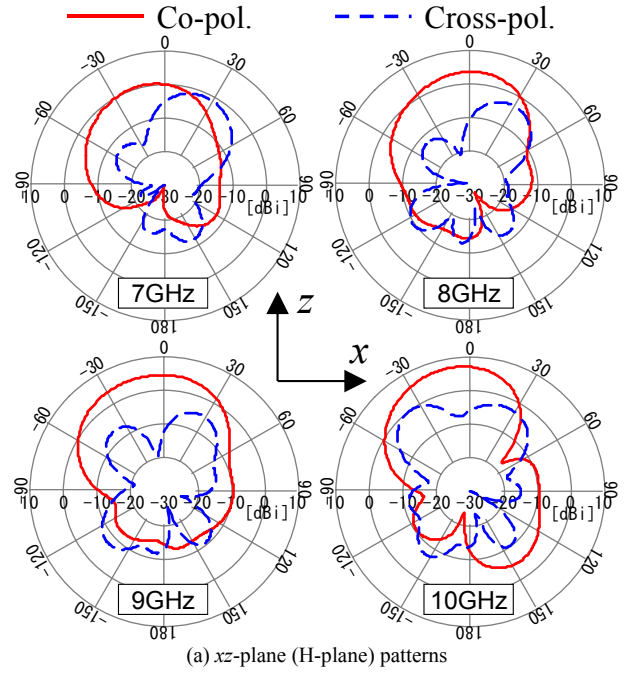
Fig. 3: Frequency response of mutual coupling.

Both monopole and notch antennas are fed by microstrip lines which are linearly tapered in order to achieve 50Ω impedance matching at each port. The strip conductors of the microstrip lines are printed on the bottom side of the substrate. For the monopole antennas, the end of the feedline is directly connected to the radiating elements. The notch antennas are connected to the end of the feedline by conducting posts. In order to obtain unidirectional radiation characteristics, a back reflector having the same dimension as those of the antenna substrate is placed underneath the antenna array.

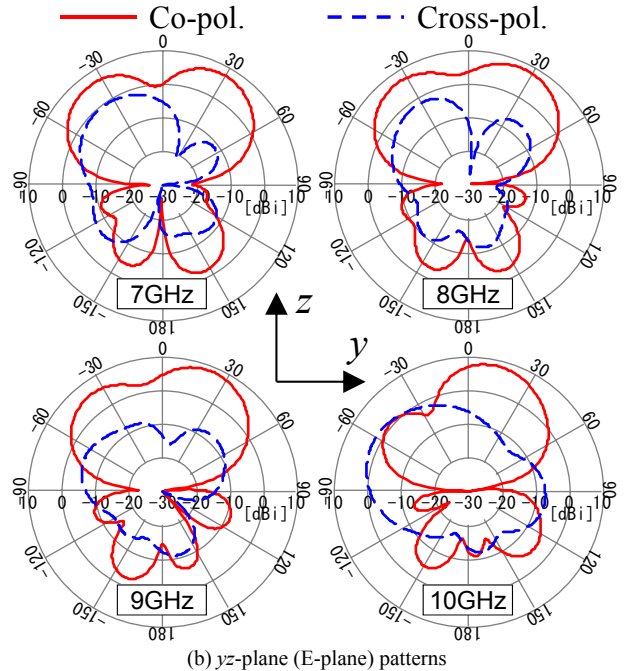
The structural parameters of the antenna assumed in the following investigations are listed in Table 1. The dimensions of the radiating elements are optimized to achieve the operation over the frequency range from 7.25GHz to 10.25GHz, which corresponds to the UWB high band in Japan. In the following considerations, the input terminals for the monopole antennas are designated as port 1 and port 3, and those for the notch antennas are designated as port 2 and port 4, as shown in Fig. 1.

III. NUMERICAL EVALUATION OF ANTENNA PERFORMANCE

Characteristics of the designed MIMO antenna array are evaluated by the FDTD analysis. In the first place, the frequency response of the reflection coefficient is evaluated for the case where the monopole (port 1) and notch (port 2) antennas are excited independently. When the port 1 or port 2 is excited, the other ports are assumed to be terminated with 50Ω loads in the simulation. The simulated results are shown



(a) xz -plane (H-plane) patterns

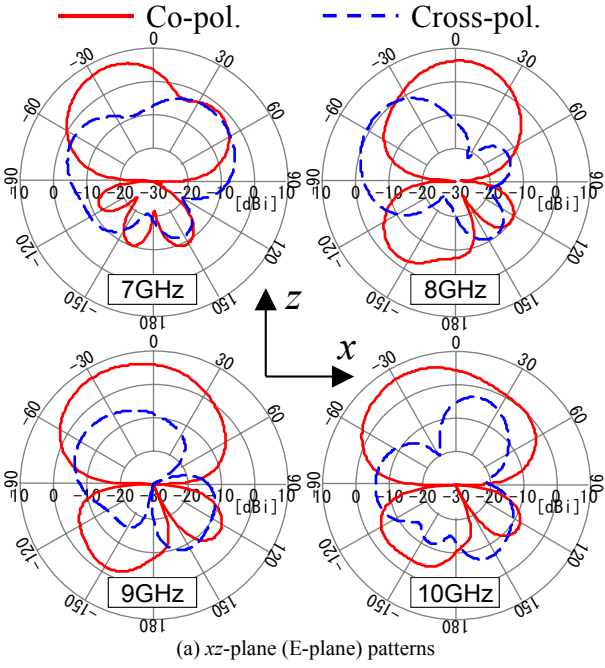


(b) yz -plane (E-plane) patterns

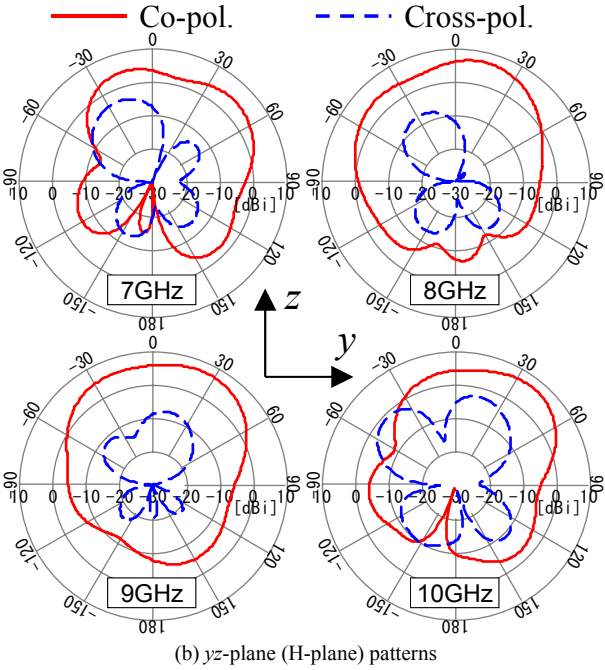
Fig. 4: Radiation patterns when port 1 (monopole antenna) is excited.

in Fig. 2. For both port 1 and port 2, the reflection coefficients are observed to be less than -10 dB.

In the next place, all mutual couplings between ports are evaluated. Fig. 3 shows the frequency response of the mutual couplings between ports 1 and 2, ports 1 and 3, ports 1 and 4, ports 2 and 4. For the case between the monopole and notch antennas ($|S_{21}|$ and $|S_{41}|$), the couplings are observed to be less than around -20 dB over the frequency range from 7.25GHz to 10.25GHz. The maximum coupling level is observed to be -12 dB for the case between the notch antennas ($|S_{42}|$).



(a) xz -plane (E-plane) patterns



(b) yz -plane (H-plane) patterns

Fig. 5: Radiation patterns when port 2 (notch antenna) is excited.

Radiation patterns for the case where one of ports is excited and the other ports are terminated with 50Ω loads have been evaluated at the frequencies of 7GHz, 8GHz, 9GHz and 10GHz. Fig. 4 and Fig. 5 shows the simulated radiation patterns for the case when port 1 and port 2 are independently excited, respectively. In these figures, solid and broken lines denote radiation patterns for co- and cross-polarization in each planes, respectively. It can be observed that the antenna exhibits quasi-unidirectional at each frequencies for the case when the port 2 excited. When the port 1 is excited, bi-directional radiation is observed in E-plane. This result may be due to the asymmetry of the antenna structure.

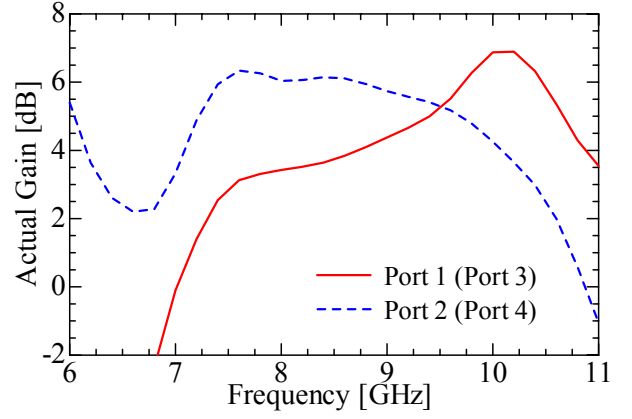


Fig. 6: Frequency response of actual gain in $+z$ -direction.

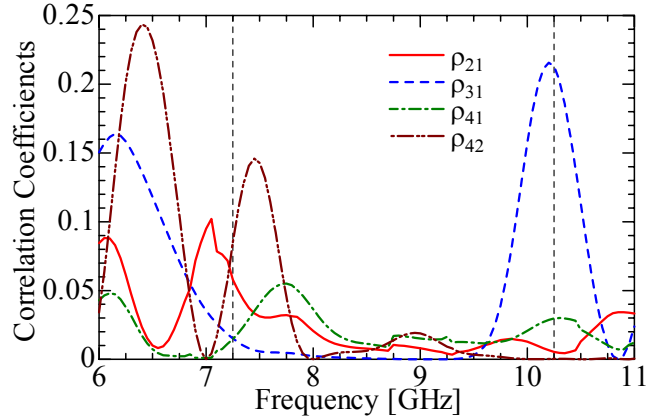


Fig. 7: Frequency response of envelope correlation coefficients.

Fig. 6 shows the frequency response of actual gain observed in $+z$ -direction. Over the frequency range from 7.25GHz to 10.25GHz, the actual gain is observed to be 2–6dBi and 3.5–6dBi for the cases when port 1 and port 2 are excited, respectively. As shown in Fig. 4(b), dimples of E-plane patterns are found in $+z$ -direction for lower frequencies. These dimples leads to the decrease of the actual gain at lower frequencies when port 1 is excited.

In order to evaluate MIMO performance of the designed antenna array, the envelope correlation coefficient among two antennas is calculated by the use of scattering parameters at each antenna port. The envelope correlation coefficient between i -th port and j -th port antennas is given by the following expression [6].

$$\rho_{ij} = \frac{|S_{ii}^* S_{ij} + S_{ji}^* S_{jj}|^2}{(1 - |S_{ii}|^2 - |S_{ji}|^2)(1 - |S_{jj}|^2 - |S_{ij}|^2)} \quad (1)$$

Fig. 7 shows the frequency response of envelope correlation coefficients that are evaluated by substituting simulated scattering parameters into the above expression (1). As suggested in [6], a good diversity effect can be obtained when the envelope correlation value is less than 0.5. As can be seen from Fig. 7, the envelope correlation values remain under 0.22 within the frequency band of 7.25–10.25GHz. This leads us to expect good performance of the proposed configuration in terms of diversity.

IV. CONCLUSIONS

A wideband 4-port MIMO antenna array has been presented in this paper. In the designed antenna array that operates over the frequency range from 7.25GHz to 10GHz, a leaf-shaped monopole and notch antennas are used as the array elements. In order to demonstrate the effective performance of the proposed configuration, characteristics of the designed MIMO antenna are evaluated numerically by the FDTD analysis. Over the frequency band of interest, the reflection coefficient is observed to be less than -10 dB and the mutual coupling between ports are less than -12 dB. The antenna port envelope correlation coefficients are observed to be less than 0.22, which are substantially smaller than the value of 0.5 being suggested for realizing the good diversity effect.

REFERENCES

- [1] S. W. Su, "High-gain dual-loop antennas for MIMO access points in the 2.4/5.2/5.8GHz bands," *IEEE Trans. Antennas Propag.*, vol.58, no.7, pp.2412-2419, July 2010.
- [2] A. Al-Rawi, J. Yang, C. Orlenius, and M. Franz'en, "The Double-sided 4-port Bow-tie Antenna: A New Compact Wideband MIMO Antenna," *Proc. Eucap 2013*, pp.3731-3735, April 2013.
- [3] C. -X. Mao and Q. -X. Chu, "Compact Coradiator UWB-MIMO Antenna With Dual Polarization," *IEEE Trans. Antennas Propag.*, vol. 62, no. 9, pp.4474-4480, Sept. 2014.
- [4] M. Ameya, M. Yamamoto, and T. Nojima, "An Omnidirectional UWB Printed Dipole Antenna with Small Waveform Distortion", *Proc. of Progress In Electromagnetics Research Symposium 2006*, 4P3, p.515, Aug. 2006.
- [5] S. Fujita, M. Yamamoto, and T. Nojima, "A Study of a Leaf-Shaped Bowtie Slot Antenna for UWB Applications," *Proc. of 2012 International Symposium on Antennas and Propagation*, 3B3-1, pp.830-833, Nov. 2012.
- [6] T.S.P. See, A.M.L. Swee, and Z.N. Chen, "Correlation analysis of UWB MIMO antenna system configurations," *Proc. of IEEE Int. Conf. on Ultra Wideband*, vol.2, pp.105-108, 2008.